Macromolecules

ARTICLE

pubs.acs.org/Macromolecules

Spectroscopic Study on Water Diffusion in Poly(L-lactide)−Poly(ethylene glycol) Diblock Copolymer Film

Ying Jin, Wei Wang, and Zhaohui Su*

State Key Laboratory of Polymer Physics and Chemistry, Changchun Institute of Applied Chemistry, Chinese Academy of Sciences, Changchun 130022, P. R. China

Supporting Information

ABSTRACT: Diffusion of water in a phase-separated poly(L-lactide)-*b*-poly(ethylene glycol) (PLLA−PEG) copolymer with both blocks crystallizable was investigated using time-resolved ATR-FTIR with deuterated water and 2D correlation analysis. Water molecules of three different states were identified in the copolymer matrix, and their formation sequence was determined. Perturbation of water on the copolymer structure was revealed. While the amorphous PLLA chains were not affected, upon water penetration, conformation distribution of crystalline PLLA chains was altered, which can be reversed upon removal of the water, and the PEG crystallinity in the copolymer was gradually destroyed and the process was not reversible. For the double amorphous PLLA−PEG film, water first associated with the more hydrophilic PEG chains and then interacted with the PLLA segments. For the double crystalline film, however, crystalline PLLA segments were first perturbed by the water before the crystalline PEG was affected. Finally, the water diffusion coefficient for the PLLA−PEG copolymer was measured and compared with that of the PLLA and PEG homopolymers.

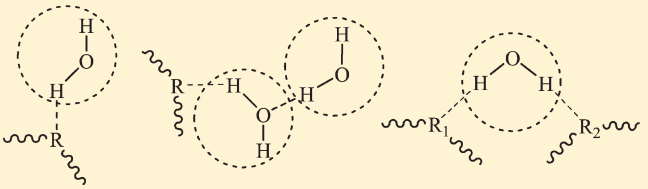

INTRODUCTION

Water is one of the simplest and yet most significant molecules. It is often present in ambience where polymer materials are in service. In this process water can adsorb to the polymers, exhibiting different structure from bulk water and affecting the physical and mechanical properties of the materials. While the diffusion and structure of water in homopolymers have been studied extensively,[1−7] in copolymers water diffusion is more complicated because of their more complex morphological structures due to phase separation and segregation. Previous work on water diffusion into copolymers has mainly focused on permeability and structure/property relationships of the polymers.[8−10] Recently, we studied the diffusion of water in an amorphous poly(ester urethane) block copolymer and identified different modes of molecular interaction between water and the hard and soft segments.[11] This work also reveals that the dynamics of water diffusion in copolymer matrix are complicated due to presence of different phase domains,[11] and more extensive research is called for to better understand the diffusion of water in phase-separated copolymer matrices. In particular, many copolymer materials of practical significance comprise blocks that can crystallize, and water diffusion in phase-separated and semicrystalline matrices is yet to be investigated.

Poly(L-lactide) (PLLA) is a biodegradable semicrystalline polymer that has attracted much attention in recent years. Its hydrophobicity, brittleness, and stiffness have considerably restricted its application.[12] To modify the physical properties and biodegradability of PLLA, other components have been incorporated.[12] Poly(ethylene glycol) (PEG) has the advantages of hydrophilicity, excellent biocompatibility, and low immunogenicity and has been used in biomedical applications to increase the stability of blood contacting materials.[13,14] Block copolymers of PLLA and PEG offer a unique combination of controlled biodegradability, biocompatibility, and hydrophilicity and do not have adverse effects on blood and tissues, and the PEG can reduce the brittleness of the material. Both blocks can crystallize under suitable conditions. PLLA−PEG block copolymers have been well studied and found applications in biomedical and pharmaceutical fields.[13−16] As biomedical materials, PLLA−PEGs are widely used in surroundings containing water, and water molecules can penetrate into the polymer matrices. The sorbed water interacts with the copolymer and modifies its chemical and physical properties. The ester linkages in the PLLA can hydrolyze, resulting in degradation,[17] and the hydrophilic PEG block increases the degradation rate.[18] Therefore, sorption of water is an important factor that influences the performance of these materials.

Attenuated total reflection Fourier transform infrared (ATR-FTIR) spectroscopy has proved to be a convenient, rapid, and accurate technique for probing dynamic diffusion behavior of small molecules through polymer films.[3,19−25] Two-dimensional (2D) correlation spectroscopy can enhance spectral resolution of

Received: October 5, 2010
Revised: February 16, 2011
Published: March 14, 2011

ACS Publications © 2011 American Chemical Society

dx.doi.org/10.1021/ma200062t | *Macromolecules* 2011, 44, 2132–2139

highly overlapped FT-IR bands[26−28] and provide specific sequences of certain spectral intensity changes taking place during the development of a significant controlling physical variable in dynamic analyses.[26,28−30] 2D correlation analysis in conjunction with ATR-FTIR has been applied to study water diffusion in various polymer matrices.[4,7,11,19,23,29,31]

In the present work, we monitor the absorption process of deuterated water in films of PLLA−PEG diblock copolymer by ATR-FTIR and investigate the interactions between water and the two components of the copolymer in order to understand the effects of water on the structure of the copolymer matrix as well as the influence of the polymer crystallinity on the diffusion process. The diffusion coefficients of water in the copolymer films are also determined.

EXPERIMENTAL SECTION

Sample Preparation. PLLA−PEG diblock copolymer[32] was kindly provided by Prof. Jing. The molecular weights of the PLLA and PEG blocks were 15K and 5K, respectively. PLLA was a commercial product purchased from Natureworks (PLA 4032D, 98% L-lactide content, $M_w \sim$ 250K, and polydispersity 1.70) and used as received. PEG (M_w = 100K) was purchased from Aldrich and used as received. Because the interactions studied by vibrational spectroscopy between water and functional units of the polymers are localized, the difference in molecular weight among the samples was not expected to cause significant impact on the results and key conclusions in our study. Solutions were prepared by dissolving the polymers in dichloromethane at a concentration of 10% (w/v). Dichloromethane was purchased from Beijing Chemicals Co. (China) and used as received. Films were prepared by casting solutions on clean glass slides or KBr tablets and dried for 36 h at room temperature to remove the residual solvent. The films cast on glass substrates were peeled off for IR analysis. A PLLA−PEG copolymer film cast on KBr tablet was placed in a Linkam THMS 600 hot stage under a nitrogen atmosphere, heated to 200 °C for complete melting, and then quickly cooled to 120 °C and maintained for 90 min. Then the temperature was decreased to 30 °C and maintained for 30 min. These crystallization conditions were determined based on a previous study[32] and our DSC analysis, and the PEG and PLLA crystallinity in this film was 30% and 48%, respectively (Figures S1 and S2, Supporting Information). The crystalline morphology of this copolymer has been studied in great detail previously.[32] The KBr tablet was dissolved from the bottom by water, and the film was collected after the KBr substrate was completely dissolved in less than 1 min. The film was quickly placed on a tissue to remove water on the surface and then dried under vacuum. Extreme caution was taken so that contact between the film and water in this process was minimized. On the basis of our later experiments (e.g., Figure S7, Supporting Information), the very short exposure of the film to water in this process did not cause any detectable structural change and had no impact on our subsequent water diffusion analysis. Before all the measurements, films were maintained under vacuum for 24 h at room temperature. Deuterium oxide (D, 99.9%, Aldrich) and ultrapure water (18.2 MΩ·cm) obtained from a Millipore Simplicity unit were used for water diffusion studies.

Time-Resolved ATR-FTIR Spectroscopy. The thicknesses of all the films were greater than 10 μm. Time-resolved ATR-FTIR measurements were carried out on a Bruker Vertex 70 FTIR spectrometer equipped with a DTGS detector and an ATR accessory (ZnSe crystal, 45°). The ATR crystal covered by a polymer film with several overlaying filter papers was mounted in the ATR cell, as shown in Scheme 1, and then 50 μL of deuterium oxide or water were injected into the filter paper while data acquisition was initiated. For each spectrum 16 scans were coadded, with a 15 s time interval before the next spectral acquisition. All spectra were collected at 4 cm^{-1} resolution in the range of 4000−650 cm^{-1}. They were baseline-corrected using OPUS 5.0 software. Curve fitting was performed using the Levenberg−Maquardt least-squares algorithm routine of the OPUS software package, and the residual rms error was about 0.001.

Scheme 1. Schematic Illustration of the ATR-FTIR Experimental Configuration

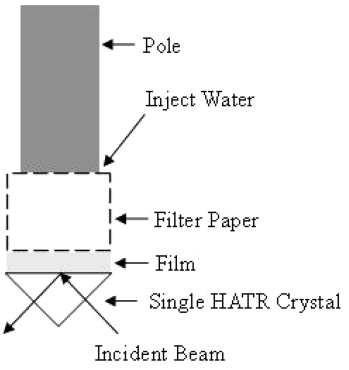

2D Correlation Analysis. Several spectra at equal time intervals and in a certain wavenumber range were selected for 2D correlation analysis using the 2D Pocha software composed by Daisuke Adachi (Kwansei Gakuin University). Time-averaged 1D reference spectra are shown at the side and top of the 2D correlation maps for comparison. In the 2D correlation maps, unshaded regions indicate positive correlation intensities, whereas shaded regions are defined as negative ones.

Estimation of Diffusion Coefficient. Normal water was used for these experiments. For Fickian diffusion in polymers, the equation is given to estimate the effective diffusion coefficient of water from ATR-FTIR spectra as follows:[25]

$$\frac{A_t}{A_\infty} = 1 - \frac{8\gamma}{\pi[1-\exp(-2\gamma L)]} \sum_{n=0}^{\infty}\left[\frac{\exp(g)[f\exp(-2\gamma L)+(-1)^n(2\gamma)]}{(2n+1)(4\gamma^2+f^2)}\right]$$

$$g = \frac{-D(2n+1)^2\pi^2 t}{4L^2},$$

$$f = \frac{(2n+1)\pi}{2L}, \quad \gamma = \frac{2\pi n_1(\sin^2\theta - {n_{21}}^2)^{1/2}}{\lambda}$$

In this equation, A_t is the absorbance of the characteristic band of water at time t, A_∞ is the band intensity at equilibrium, γ is the reciprocal of the penetration depth of the evanescent wave, L is the thickness of the polymer film (invariable), and D is the diffusion coefficient. For water diffusion measurements using our ATR setup, the penetration depth (d_p) at 3300 cm^{-1} (where the O−H stretching band centers) was about 0.58 μm according to the following equation: $d_p = \lambda/(2\pi n_1(\sin^2\theta - {n_{21}}^2)^{1/2})$, where λ is the wavelength of the radiation in air, θ is the incidence angle, n_1 is the refractive index of the ATR crystal, and n_{21} is the ratio of the refractive index of the polymer to that of the ATR crystal. The penetration depth was much smaller than the thickness of the film (>10 μm) and can be assumed constant during the diffusion process, meeting the requirement of diffusion coefficient calculation.[25] The diffusion coefficient was calculated by a nonlinear curve-fitting[23] to the equation from the variation of the $\nu_{(OH)}$ stretching band area versus time. For each sample, three replicate films were prepared separately and analyzed, and the results were averaged.

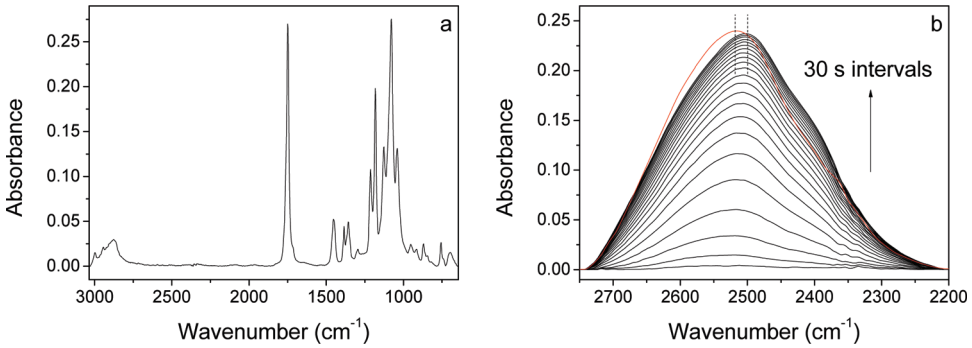

Figure 1. (a) ATR-FTIR spectrum of a dry amorphous PLLA−PEG film. (b) Time-resolved spectra in the region of 2750−2200 cm^{-1} for deuterated water diffusion into amorphous PLLA−PEG film (black) and a spectrum for deuterated water diffusion into crystalline PLLA−PEG film at steady state (red). The dotted lines indicate the band maximum position for the two films at steady state.

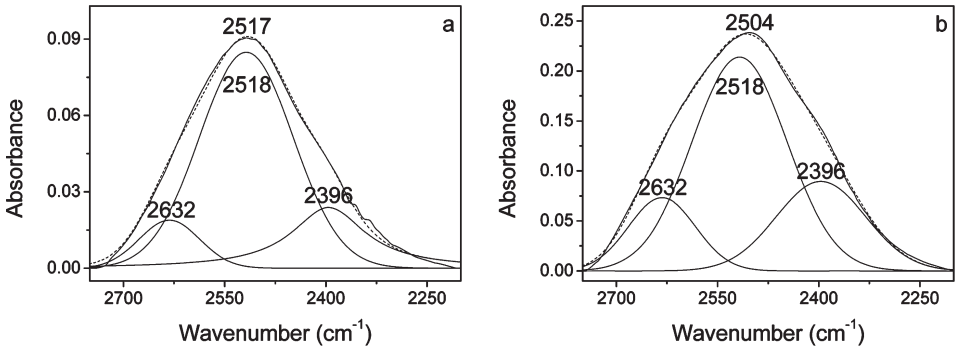

Figure 2. Peak fitting of the infrared band in the range of 2750−2200 cm^{-1} of deuterated water in the PLLA−PEG film at early stage (a) and steady state (b) of the diffusion.

RESULTS AND DISCUSSION

Both PLLA and PEG homopolymers can readily crystallize under suitable conditions. For the PLLA−PEG film cast directly from solution, both PLLA and PEG were amorphous as indicated by wide-angle X-ray diffraction and FTIR (Figures S3 and S4, Supporting Information). ATR-FTIR analysis can provide real-time information on water in polymer film within a certain depth. An ATR-FTIR spectrum of the dry PLLA−PEG film is shown in Figure 1a. Time-resolved ATR-FTIR spectra in the range of 2750−2200 cm^{-1} for the absorption of deuterated water into the double amorphous PLLA−PEG film are shown in Figure 1b. The infrared band, assigned to the stretching vibration of the O−D group in deuterated water ($\nu_{(OD)}$), is observed to gradually increase and seems to shift toward lower wavenumbers as a function of time when deuterated water diffuses into the film. The same band observed for diffusion into double crystalline PLLA−PEG at steady state is also included for comparison, which occurs at higher wavenumbers than that for the amorphous film. As is well-known, O−H stretching vibrations in water are predicted to exhibit sequential red shift with increasing strength of the hydrogen bond. Thus, the frequency difference for the O−D stretchings between the two cases suggests that the hydrogen-bonding interactions of water with the amorphous polymer are stronger than that with the crystalline one, which may be attributed to greater chain segment mobility and more sites available in the amorphous polymer that favor the formation of strong hydrogen bonds.

The broad $\nu_{(OD)}$ band of deuterated water in this region is not interfered by vibrational bands of the polymer. Peak fitting of the band is shown in Figure 2, and three components located at around 2400, 2520, and 2630 cm^{-1} are readily identified. It is obvious that the component at ~2400 cm^{-1} increased with time while the one at ~2520 cm^{-1} decreased, leading to shift of the profile maximum of the broad band toward lower wavenumbers. Because of uncertainty in peak fitting processes, to validate these components, 2D analysis was performed.

Figure 3 shows the 2D asynchronous correlation spectra of the deuterated water absorbed in the PLLA−PEG film in the same spectral range of 2750−2200 cm^{-1}. It reveals that the broad O−D stretching band comprises three separate components, located at ~2400, 2530, and 2650 cm^{-1}, which is consistent with and supports the above finding from peak fitting shown in Figure 2. The peak fitting and 2D analysis results suggest that there are three different states of water in the film. The three components correspond to the absorbance from strongly hydrogen-bonded, medium hydrogen-bonded hydroxyl groups, and weak hydrogen-bonding interactions, respectively. More specifically, the band at 2400 cm^{-1}, the lowest component, indicates strong hydrogen-bonding interactions between hydrophilic groups of the polymer and the deuterated water molecules, the band at 2530 cm^{-1} is associated with moderate hydrogen-bonding interactions between the hydrophilic groups and the deuterated water molecules, and the absorption at the highest frequency (2650 cm^{-1}) belongs to the deuterated water residing in free volume (microvoids) with little or no hydrogen bonding between each other as well as water forming weak hydrogen bonds with the polymer (more detailed discussion on these structures in next section).

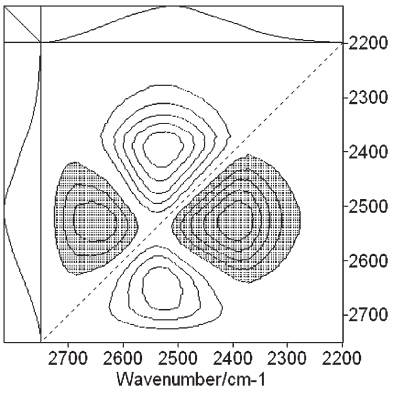

Figure 3. Asynchronous 2D FT-IR correlation spectra of deuterated water diffusion into the PLLA−PEG film in the range of 2750−2200 cm^{-1}.

In 2D correlation spectra, $\varphi(\nu_1,\nu_2)$ and $\psi(\nu_1,\nu_2)$ represent the cross-peaks between ν_1 and ν_2 in synchronous and asynchronous correlation spectra, respectively. $\varphi(\nu_1,\nu_2)$ indicates the overall similarity between two separate spectral intensity variations measured at different spectral variables, while the appearance of an asynchronous correlation peak, $\psi(\nu_1,\nu_2)$, may be regarded as a measure of dissimilarity of the spectral intensity variations and indicates that the bands ν_1 and ν_2 vary out of phase with each other during the diffusion process. The sign yields information about the sequential order of intensity changes between band ν_1 and band ν_2. According to the rules proposed by Noda,[26] if $\varphi(\nu_1,\nu_2) > 0$, $\psi(\nu_1,\nu_2)$ is positive (unshaded area), band ν_1 varies before band ν_2 does, and if $\psi(\nu_1,\nu_2)$ is negative (shaded area), which implies the opposite phenomena, band ν_1 varies after band ν_2 does. If $\varphi(\nu_1,\nu_2) < 0$, this rule is reversed. In the 2D synchronous correlation spectra of the deuterated water absorbed in the PLLA−PEG film in the spectral range of 2750−2200 cm^{-1}, the cross-peak is positive (Figure S5, Supporting Information), which means that all the components increase with time during the diffusion process. In Figure 3, the positive peak ψ(2530,2400) suggests that the band at 2530 cm^{-1} varies prior to the band at 2400 cm^{-1}, and the negative asynchronous cross-peak located at 2650/2530 cm^{-1} reveals that the band at 2650 cm^{-1} varies later than the band at 2530 cm^{-1}. Therefore, the sequence of the spectral changes is obtained from asynchronous 2D ATR-FTIR correlation spectra by judgment of the sign of the correlation peak, which is as follows: 2530 → 2650 and 2400 cm^{-1} for deuterated water diffusion in the PLLA−PEG film. Furthermore, it is known that carbonyl and oxygen can form weak (−O−*HOH*), moderately strong (−CO−*HOH*, −CO−HOH−*HOH*, −O−HOH−*HOH*), and strong hydrogen bonds (−CO−*HOH*−CO−, −CO−*HOH*−HOH, −O−*HOH*−O−, −CO−*HOH*−O−) with water.[3,5,31,33] By combining these structures with our analyses on the spectroscopic data discussed above, as shown in Figure 4, we can conclude that when water diffuses into PLLA−PEG films, the water is moderately bound to the polymer first, by preferentially forming hydrogen bonds with the C═O and the −O− groups. Then, water molecules diffuse into free volume (microvoids) in the polymer, forming water clusters, as well as into the polymer network, forming weak and strong hydrogen bonds with the polymer.

After investigating the various structures of water formed in the diffusion process, we turn our attention to the effects of water on the polymer structure by studying the characteristic bands of

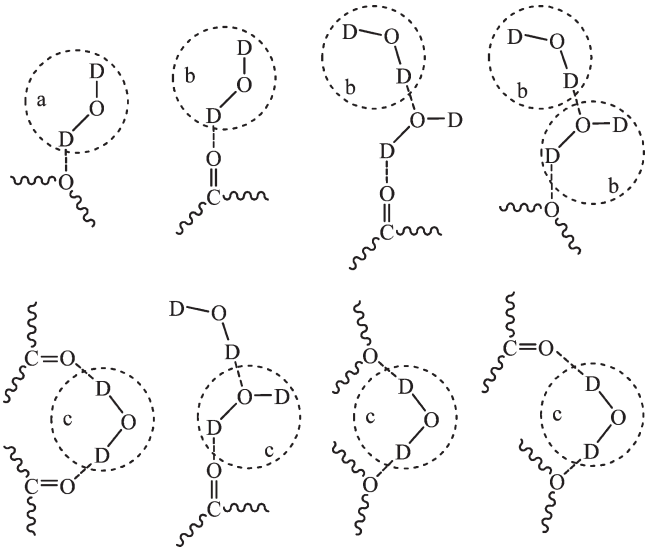

Figure 4. Interactions between deuterated water and PLLA−PEG: weak (a), moderately strong (b), and strong (c) hydrogen bonds.

the polymer. According to literature,[34] the carbonyl stretching band of PLLA at 1790−1730 cm^{-1} is composed of four components at about 1776, 1767, 1759, and 1749 cm^{-1}. The bands at 1776, 1767, and 1749 cm^{-1} are attributed to *gg*, *tg*, and *tt* conformers, respectively, primarily due to intramolecular coupling, while the band at 1759 cm^{-1} corresponds to the overlapped absorption of *gt* conformers in the amorphous and crystalline phases.[34] For the amorphous film, the shape of this carbonyl stretching band was found to be the same before (dry) and after (wet) the deuterated water diffusion (Figure 5a), indicating that the conformation distribution of the amorphous polymer chains did not change with the inclusion of water, even though water forms hydrogen bonds with the polymer. For the crystalline film, however, pronounced splitting and broadening of the carbonyl band, shown in Figure 5b, is observed in both dry and wet states, presumably due to the addition of the crystalline component. Furthermore, the band broadening and splitting are reduced at the wet state compared to the dry one, as seen in Figure 5b, suggesting a variation in conformation distribution in the crystalline film with water sorption. The composition of the carbonyl band was analyzed via band deconvolution (Figure S6, Supporting Information). It was found that the area fraction of the component at 1759 cm^{-1}, associated with the crystalline phase, was 33% in dry state, and it decreased to 29% after water uptake. Then upon redrying of the wet film, the carbonyl band was observed to regain its shape as that of the dry film, and the area fraction of the component at 1759 cm^{-1} went up to ∼33% again (Figure S6, Supporting Information). These results suggest that although the PLLA crystalline region is difficult to be penetrated by water molecules, part of the crystalline chains, probably the segments in the interphase between the crystalline and the amorphous, can still interact with the water molecules, resulting in conformation change of the polymer chains, and the conformation change is reversible upon removal of the water. The synchronous and asynchronous 2D FT-IR correlation spectra of the crystalline PLLA−PEG film in the range of 1790−1730 cm^{-1} for the water diffusion process are shown in Figure 6. The cross-peaks in the synchronous map are positive, while in the asynchronous map the peak at ψ(1757,1748) is

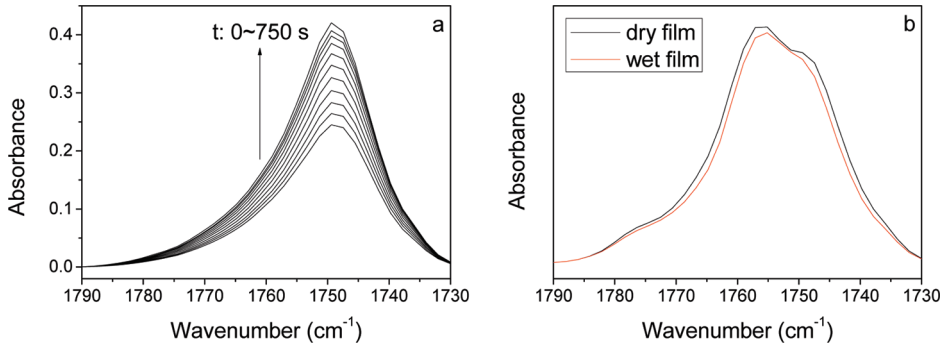

Figure 5. ATR-FTIR spectra in the region of 1790−1730 cm^{-1} for deuterated water diffusion into amorphous (a) and crystalline (b) PLLA−PEG films.

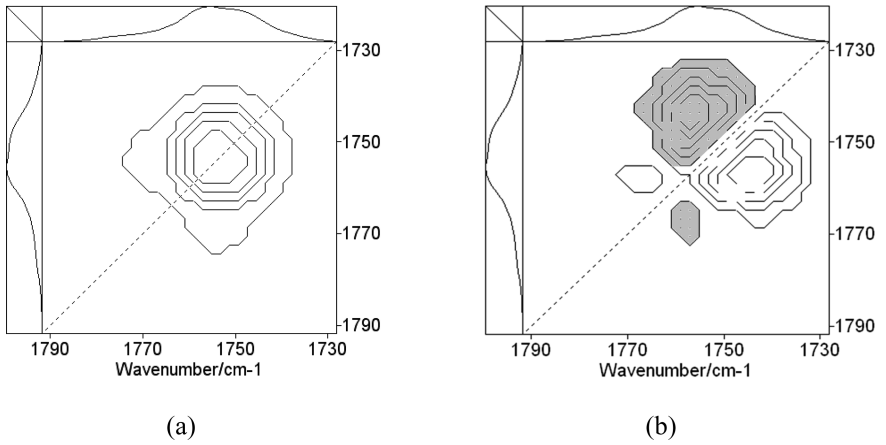

Figure 6. Synchronous (a) and asynchronous (b) 2D FT-IR correlation spectra of water diffusion into the crystalline PLLA−PEG film in the range of 1790−1730 cm^{-1}.

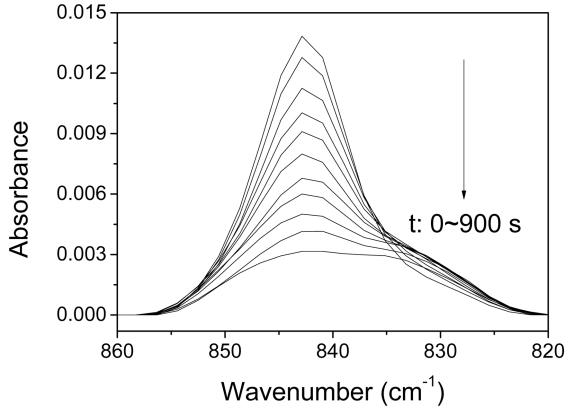

Figure 7. Variation of the PEG crystalline band in the range of 860−820 cm^{-1} during the process of water diffusion into a crystalline PLLA−PEG film.

negative and the peak at $\psi(1767,1757)$ is positive. These mean that the peaks at 1748 and 1767 cm^{-1} change before the one at 1757 cm^{-1}. According to the assignments of the components of the carbonyl stretching band, it is evident that the amorphous carbonyl changes before the crystalline carbonyl does; i.e., water molecules first form hydrogen bonds with the amorphous carbonyls and then diffuse into the crystalline domains and interact with the crystalline carbonyl groups.

In the spectrum of the PLLA−PEG copolymer, the band at ∼843 cm^{-1} is associated with the combination of CH_2 rocking and COC deformation of PEG and is sensitive to conformational order.[35−37] This peak is characteristic of PEG crystallinity.[35−37] In the process of water diffusion into the crystalline PLLA−PEG diblock copolymer, it can be seen that the intensity of the PEG crystalline peak at 843 cm^{-1} decreases significantly and the sharp peak becomes a broad band with water uptake (Figure 7). It suggests that the crystalline domains of PEG in the diblock copolymer are destroyed gradually and the stable conformation is reduced.[35−37] Obviously, this is due to the hydrophilicity and water solubility of PEG. Unlike the reversible effects of water on the PLLA domains, this disruption of the PEG crystallinity was found to be irreversible upon removal of water from the film.

Then we investigate the diffusion process via time-resolved FTIR spectroscopy. Figure 8a displays the evolution of the PLLA $\nu_{(CO)}$ band at ∼1750 cm^{-1} and the $-CH_2-$ stretching bands at 2930−2780 cm^{-1} characteristic of PEG[36,38] for the amorphous PLLA−PEG film over the diffusion process, and the intensity variations of the two bands are plot in Figure 8b as functions of time, which indicate that the amorphous PEG block changes before the amorphous PLLA does. The data were also analyzed using 2D correlation analysis. Figure 9 shows the 2D correlation spectra of double amorphous PLLA−PEG film during water diffusion in the range of 2930−2780 cm^{-1} vs 1790−1730 cm^{-1} to correlate the band intensity changes of $\nu_{(CH2)}$ (associated with

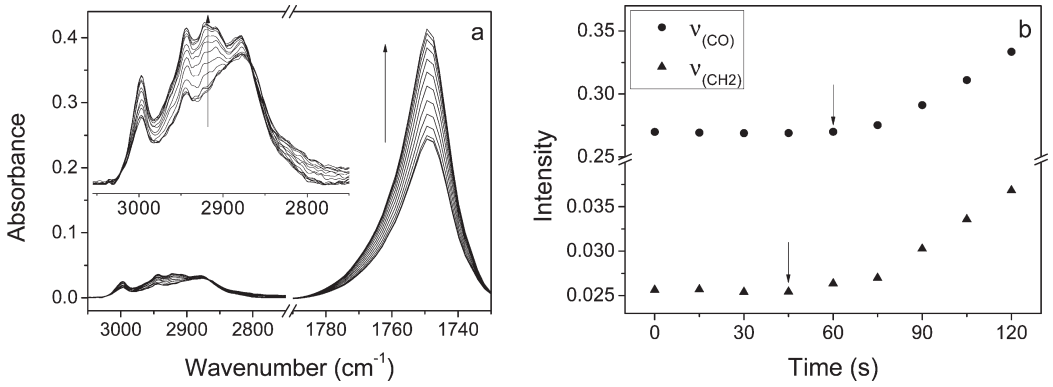

Figure 8. (a) Time-resolved FTIR spectra of amorphous PLLA−PEG film over deuterated water diffusion process (inset is the magnification of the C−H stretching region, and arrows represent increasing time). (b) Band intensity as a function of time for $\nu_{(CO)}$ (PLLA) and $\nu_{(CH2)}$ (PEG) (arrows indicate the starting points of the represented events).

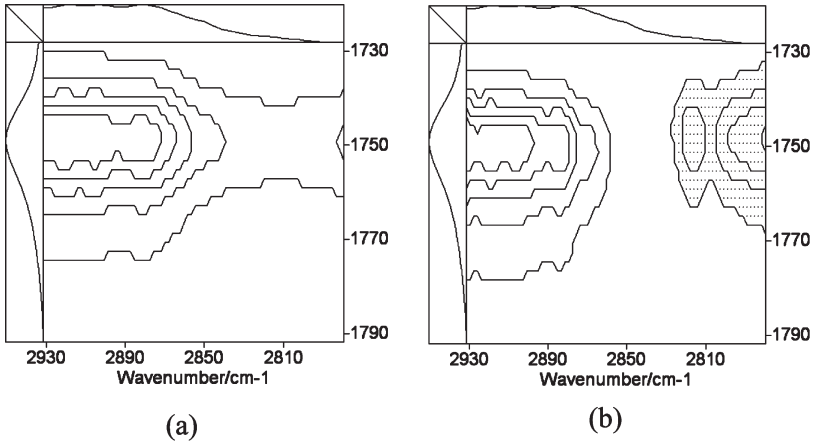

Figure 9. Synchronous (a) and asynchronous (b) 2D FT-IR correlation spectra of the amorphous PLLA−PEG film during water diffusion in the range of 2930−2780 cm^{-1} vs 1790−1730 cm^{-1}.

the PEG block) and $\nu_{(CO)}$ (representing the PLLA). The two positive peaks $\varphi(2910,1750)$ and $\psi(2910,1750)$ confirm that the band at 2910 cm^{-1} varies before the band at 1750 cm^{-1}; i.e., the amorphous PEG block changes before the amorphous PLLA block during the diffusion process. This probably is due to the hydrophilicity difference of the two components. When water enters the double amorphous copolymer matrix, it tends to associate with the more hydrophilic PEG segments first before interacting with the PLLA segments.

However, the sequence was found to reverse for water diffusion into double crystalline PLLA−PEG matrix. Figure 10 shows the 2D spectra correlating the same two spectral regions associated with PLLA and PEG over the water diffusion into the double crystalline PLLA−PEG film. The two (2890, 1750) cross-peaks in the synchronous and asynchronous spectra are negative and positive, respectively, indicating that the band at 1750 cm^{-1} due to PLLA varies before the band at 2890 cm^{-1} associated with PEG. To further verify this result, correlation between the spectral range of 1790−1730 cm^{-1} vs 860−820 cm^{-1}, where a band characteristic of PEG crystallinity is present, was analyzed for the water diffusion, and the contour maps are shown in Figure 11. The cross-peaks at (1750, 843) in the synchronous and asynchronous maps are both negative, revealing that the PLLA carbonyl stretching band varies before the PEG crystalline band at 843 cm^{-1}. Thus, 2D correlation analyses for two different spectral regions both demonstrate that the crystalline PLLA block changes before the crystalline PEG block during the diffusion process. This was also verified by time-resolved 1D spectra (Figure S7, Supporting Information), which revealed that water interacts with the two blocks and the PEG crystalline structure is destroyed gradually, and the PLLA block changes before the PEG block does. This reversed sequence compared to that occurs in the amorphous film may be attributed to the morphology of the film. Previous study indicates that when this particular copolymer, with 75 wt % PLLA, is cooled down from melt, PLLA crystallizes first, and then PEG crystallizes at lower temperature under the confinement of the PLLA crystalline domains.[39] In addition, PEG crystals are more compact than PLLA crystals.[39] Therefore, the crystalline PEG domains in the double crystalline copolymer film are less accessible than the PLLA, and water molecules first interacts with PLLA segments before with PEG segments when entering the crystalline PLLA−PEG film.

We also prepared film samples with one block being amorphous and the other crystalline by controlling the crystallization conditions and investigated the interaction sequence of water with the two components using the same 2D analysis approach. In both cases it was found that the interactions between water and the amorphous component occur first (data not shown).

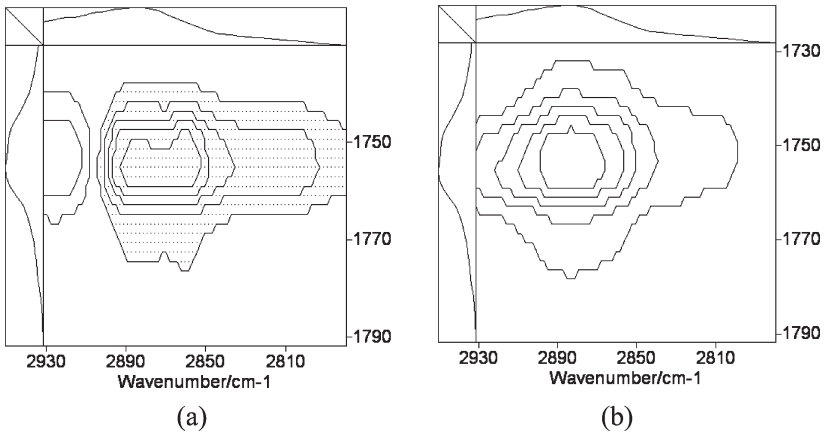

Figure 10. Synchronous (a) and asynchronous (b) 2D FT-IR correlation spectra of the double crystalline PLLA−PEG film during water diffusion in the range of 2930−2780 cm^{-1} vs 1790−1730 cm^{-1}.

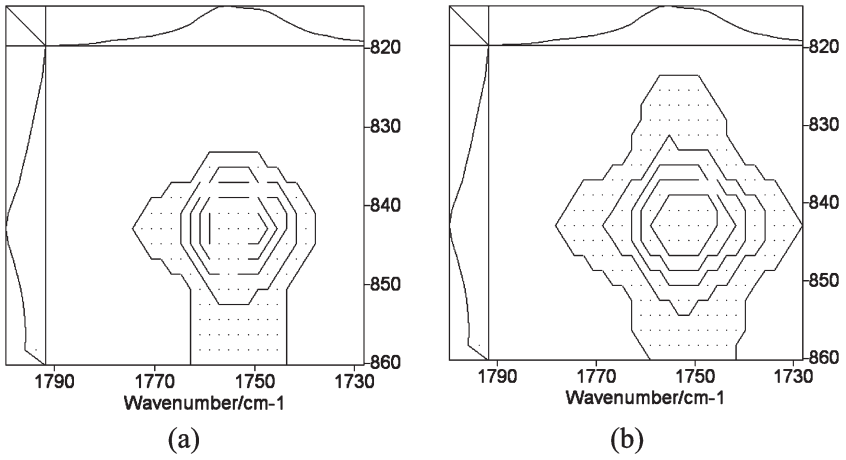

Figure 11. Synchronous (a) and asynchronous (b) 2D FT-IR correlation spectra of the double crystalline PLLA−PEG film during water diffusion in the range of 1790−1730 cm^{-1} vs 860−820 cm^{-1}.

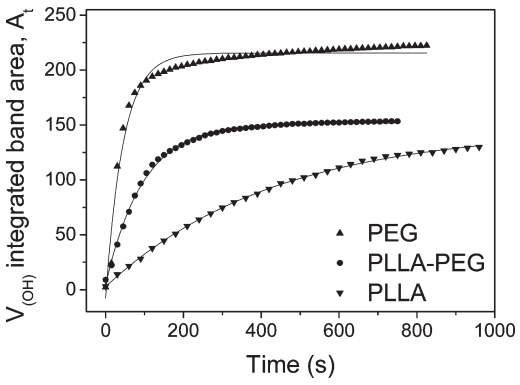

Figure 12. Integrated intensity of $\nu_{(OH)}$ as a function of time for water diffusion in amorphous PLLA and PLLA−PEG, and quenched PEG films.

It has been reported that diffusion coefficient of water in polymer matrix can be measured via the time-resolved ATR-FTIR spectroscopy technique.[25] Following this approach, the diffusion coefficients of water in the amorphous PLLA and PLLA−PEG and quenched PEG films were measured. The integrated intensity of the $\nu_{(OH)}$ band over the diffusion process as a function of time is plotted for the three films respectively in Figure 12. It is clear that the amount of water in the PEG film goes up most rapidly and reaches the highest plateau value at long time, indicating that water diffuses fastest in PEG, and the matrix can absorb more water than the other two polymers. The band intensity increases the slowest over time for the PLLA film and reaches the lowest plateau value, with the PLLA−PEG copolymer in between the two homopolymers. A diffusion coefficient can be derived from each by curve fitting as described in the Experimental Section. The average diffusion coefficient obtained for the amorphous PLLA, PLLA−PEG, and PEG films was $(1.4 \pm 0.12) \times 10^{-9}$, $(9.2 \pm 3.5) \times 10^{-9}$, and $(4.2 \pm 1.3) \times 10^{-8}$ cm^2/s, respectively. The order of the diffusion coefficients and the maximum water uptakes is consistent with the hydrophilicity of the polymer matrices. The more hydrophilic the polymer is, the easier water penetrates the matrix, and the greater the diffusion coefficient is, and the more water the polymer can absorb. It should also be noted that attempts of measuring diffusion coefficient for crystalline PLLA and PEG and the copolymer produced numbers with poor reproducibility but in general greater than that for the corresponding amorphous films.

This unexpected result probably was due to mechanical defects in the crystalline films. While the amorphous films were rather homogeneous, in the crystalline films cracks were observed, and these cracks may have become shortcuts for the water molecules, resulting in greater diffusion coefficients than that for the respective amorphous films.

CONCLUSIONS

Water diffusion in PLLA−PEG diblock copolymer film has been investigated by 2D ATR-FTIR at the molecular level. There are three different states of water molecules in the copolymer film. Water first forms moderately strong hydrogen bonds with the ether linkages and the carbonyls. Then, water diffuses into free volume and forms weak hydrogen bonds, and strongly bounded water molecules form hydrogen bonds with two −C═O or two −O− and water clusters occur. With absorption of water, conformation distribution of crystalline PLLA chains is altered, which can be reversed upon removal of the water, while the PEG crystallinity in the copolymer is gradually destroyed and the process is not reversible; the conformation of amorphous PLLA chains are not affected in the process. For the double amorphous PLLA−PEG film, water first associates with the more hydrophilic PEG chains and then interacts with the PLLA segments. For the double crystalline film, however, crystalline PLLA segments are first perturbed by the water before the crystalline PEG is affected. These results demonstrate that morphology is critical to the diffusion of water in crystalline copolymer matrices and may help guide the design, processing, and application of PLLA−PEG diblock copolymers in various biomedical and pharmaceutical areas.

ASSOCIATED CONTENT

Supporting Information. Confirmation of crystallinity by DSC, XRD, and FTIR, synchronous 2D spectra of the O−D region, deconvolution of the carbonyl band, and time-resolved 1D FTIR data for the crystalline film. This material is available free of charge via the Internet at http://pubs.acs.org.

AUTHOR INFORMATION

Corresponding Author

*Tel (86)431-85262854; Fax (86)431-85262126; e-mail zhsu@ciac.jl.cn.

ACKNOWLEDGMENT

The authors thank Prof. Xiabin Jing for kindly providing the copolymer sample for this work. Financial support from the National Natural Science Foundation of China (20774097) is acknowledged. Z.S. thanks the NSFC Fund for Creative Research Groups (50921062) for support.

REFERENCES

(1) Weir, M. D.; Bastide, C.; Sung, C. S. P. *Macromolecules* **2001**, *34*, 4923–4926.
(2) Mijovic, J.; Zhang, H. *Macromolecules* **2003**, *36*, 1279–1288.
(3) Kitano, H.; Ichikawa, K.; Ide, I.; Fukuda, M.; Mizuno, W. *Langmuir* **2001**, *17*, 1889–1895.
(4) Musto, P.; Ragosta, G.; Mensitieri, G.; Lavorgna, M. *Macromolecules* **2007**, *40*, 9614–9627.
(5) Gemmei-Ide, M.; Motonaga, T.; Kitano, H. *Langmuir* **2006**, *22*, 2422–2425.
(6) Sammon, C.; Mura, C.; Yarwood, J.; Everall, N.; Swart, R.; Hodge, D. *J. Phys. Chem. B* **1998**, *102*, 3402–3411.
(7) Jin, Y.; Su, Z. H. *Chin. J. Appl. Chem.* **2011**, *28* (1), 16–21.
(8) Iordanskii, A. L.; Razumovskii, L. P.; Krivandin, A. V.; Lebedeva, T. L. *Desalination* **1996**, *104*, 27–35.
(9) Jonquieres, A.; Clement, R.; Lochon, P. *Prog. Polym. Sci.* **2002**, *27*, 1803–1877.
(10) Dolmaire, N.; Espuche, E.; Mechin, F.; Pascault, J. P. *J. Polym. Sci., Part B: Polym. Phys.* **2004**, *42*, 473–492.
(11) Wang, W.; Jin, Y.; Su, Z. H. *J. Phys. Chem. B* **2009**, *113*, 15742–15746.
(12) Nair, L. S.; Laurencin, C. T. *Prog. Polym. Sci.* **2007**, *32*, 762–798.
(13) Saito, N.; Okada, T.; Horiuchi, H.; Murakami, N.; Takahashi, J.; Nawata, M.; Ota, H.; Nozaki, K.; Takaoka, K. *Nature Biotechnol.* **2001**, *19*, 332–335.
(14) Gref, R.; Minamitake, Y.; Peracchia, M. T.; Trubetskoy, V.; Torchilin, V.; Langer, R. *Science* **1994**, *263*, 1600–1603.
(15) Uhrich, K. E.; Cannizzaro, S. M.; Langer, R. S.; Shakesheff, K. M. *Chem. Rev.* **1999**, *99*, 3181–3198.
(16) Jeong, B.; Bae, Y. H.; Lee, D. S.; Kim, S. W. *Nature* **1997**, *388*, 860–862.
(17) Vert, M.; Li, S. M.; Garreau, H. *J. Biomater. Sci., Polym. Ed.* **1994**, *6*, 639–649.
(18) Zhu, K. J.; Lin, X. Z.; Yang, S. L. *J. Appl. Polym. Sci.* **1990**, *39*, 1–9.
(19) Tang, B. B.; Wu, P. Y.; Siesler, H. W. *J. Phys. Chem. B* **2008**, *112*, 2880–2887.
(20) Murphy, D.; Depinho, M. N. *J. Membr. Sci.* **1995**, *106*, 245–257.
(21) Marechal, Y.; Chamel, A. *J. Phys. Chem.* **1996**, *100*, 8551–8555.
(22) Marechal, Y. *Faraday Discuss* **1996**, *103*, 349–361.
(23) Liu, M. J.; Wu, P. Y.; Ding, Y. F.; Chen, G.; Li, S. J. *Macromolecules* **2002**, *35*, 5500–5507.
(24) Ide, M.; Yoshikawa, D.; Maeda, Y.; Kitano, H. *Langmuir* **1999**, *15*, 926–929.
(25) Fieldson, G. T.; Barbari, T. A. *Polymer* **1993**, *34*, 1146–1153.
(26) Noda, I. *Appl. Spectrosc.* **1993**, *47*, 1329–1336.
(27) Noda, I. *J. Am. Chem. Soc.* **1989**, *111*, 8116–8118.
(28) Noda, I. *Bull. Am. Phys. Soc* **1986**, *31*, 520–520.
(29) Shen, Y.; Wu, P. Y. *J. Phys. Chem. B* **2003**, *107*, 4224–4226.
(30) Murayama, K.; Wu, Y. Q.; Czarnik-Matusewicz, B.; Ozaki, Y. *J. Phys. Chem. B* **2001**, *105*, 4763–4769.
(31) Wan, L. S.; Huang, X. J.; Xu, Z. K. *J. Phys. Chem. B* **2007**, *111*, 922–928.
(32) Sun, J. R.; Hong, Z. K.; Yang, L. X.; Tang, Z. H.; Chen, X. S.; Jing, X. B. *Polymer* **2004**, *45*, 5969–5977.
(33) Cotugno, S.; Larobina, D.; Mensitieri, G.; Musto, P.; Ragosta, G. *Polymer* **2001**, *42*, 6431–6438.
(34) Meaurio, E.; Zuza, E.; Lopez-Rodriguez, N.; Sarasua, J. R. *J. Phys. Chem. B* **2006**, *110*, 5790–5800.
(35) Matsuura, H.; Fukuhara, K. *J. Polym. Sci., Part B: Polym. Phys.* **1986**, *24*, 1383–1400.
(36) Shephard, J. J.; Bremer, P. J.; McQuillan, A. J. *J. Phys. Chem. B* **2009**, *113*, 14229–14238.
(37) Wahab, S. A.; Matsuura, H. *Phys. Chem. Chem. Phys.* **2001**, *3*, 4689–4695.
(38) Yoshihara, T.; Murahashi, S.; Tadokoro, H. *J. Phys. Chem.* **1964**, *41*, 2902–2911.
(39) Yang, J. L.; Zhao, T.; Cui, J. J.; Liu, L. J.; Zhou, Y. C.; Li, G.; Zhou, E. L.; Chen, X. S. *J. Polym. Sci., Part B: Polym. Phys.* **2006**, *44*, 3215–3226.